IEEE Access
Multidisciplinary ⋮ Rapid Review ⋮ Open Access Journal

Received May 24, 2022, accepted June 6, 2022, date of publication June 13, 2022, date of current version June 17, 2022.

Digital Object Identifier 10.1109/ACCESS.2022.3182338

Evaluating Performance of a Linear Hybrid State Estimator Utilizing Measurements From RTUs and Optimally Placed PMUs

MERCY NDINDA KIIO[1], (Student Member, IEEE), CYRUS WABUGE WEKESA[2], AND STANLEY IRUNGU KAMAU[3], (Member, IEEE)

[1]Department of Electrical Engineering, Pan African University Institute for Basic Sciences, Technology and Innovation, Nairobi 62000-00200, Kenya
[2]School of Engineering, University of Eldoret, Eldoret 1125-30100, Kenya
[3]Department of Electrical and Electronic Engineering, Jomo Kenyatta University of Agriculture and Technology, Nairobi 62000-00200, Kenya

Corresponding author: Mercy Ndinda Kiio (mercyndinda@gmail.com)

The work of Mercy Ndinda Kiio was supported by the Pan African University.

ABSTRACT Synchro-phasor technology, using Phasor Measurement Unit (PMU), has improved the way power system data is collected for monitoring through state estimation. The placement of PMUs in a power system presents technical benefits, but it comes with high infrastructural costs. It is, therefore, necessary to install the minimum number of PMUs at optimal locations subject to power system observability, creating the Optimal PMU Placement Problem (OPPP). Some factors may be considered constraints in the OPPP, such as PMU outage. The main challenge with incorporating such constraints in the PMU placement problem is that the minimum number of PMUs required for system observation increases, contributing to the high infrastructural costs. This paper, therefore, proposes using a Linear Hybrid State Estimator (LHSE) that considers existing Remote Terminal Unit (RTU) measurements randomly distributed within the system and optimally placed Phasor Measurement Unit (PMU) measurements. The proposed LHSE addresses challenges associated with nonlinearity in state estimation. The LHSE is also based on the Weighted Least Absolute Value (WLAV) criterion, considered robust and able to detect and discard bad data during the estimation process. The proposed LHSE can address state estimation reliability and resiliency, specifically the PMU outage contingency, by employing existing RTU measurements and optimally placed PMU measurements based on the Artificial Bee Colony (ABC) optimization technique. The proposed approach also leverages RTU and PMU measurements to address PMU loss contingency instead of utilizing PMU measurements only as in existing studies. Three test cases (IEEE 14 Bus, IEEE 30 Bus, and IEEE 57 Bus) are considered, with the simulations performed in MATLAB using MATPOWER data. The performance of LHSE is evaluated considering PMU/RTU measurements and PMU measurements only scenarios. Both RTU/PMU measurements present a lower Normalized Cumulative Error (NCE) performance index than PMU measurements only. In case of a single PMU outage, the proposed LHSE can estimate all states based on RTU/PMU measurements instead of only PMU measurements that fail.

INDEX TERMS Linear hybrid state estimator, optimal PMU placement, phasor measurement unit, remote terminal unit, PMU outage.

I. INTRODUCTION

State estimation, a key function served by an energy control center, is essential for the real-time monitoring of a power system [1]. Conventionally, state estimators rely heavily on measurements obtained through the Supervisory Control and Data Acquisition (SCADA) system, using Remote Terminal Units (RTUs) to measure power injections at buses and power flows through the transmission lines, and voltage magnitude at the system buses. Some of the inadequacies associated with RTU measurements include low resolution and unsynchronized measurements that cannot capture the real-time dynamics of a power system [2]. With synchro-phasor technology, modern state estimators can use Phasor Measurement

The associate editor coordinating the review of this manuscript and approving it for publication was Ziang Zhang.

Units (PMUs) data for state estimation, such as voltage and current phasors. PMUs can also measure the frequency and rate of change of frequency of the electrical signals using a source of time synchronization, the global positioning system. On top of state estimation, PMU data has a wide range of applications in real-time operations of power transmission systems [3].

The integration of RTU and PMU measurements results in a Hybrid State Estimator (HSE) associated with various formulation challenges. First, an iterative state estimation algorithm is used due to the nonlinearity posed by RTU measurements, resulting in initialization, convergence, and computational burden challenges. Second is the inclusion of PMU current phasor in the measurement vector since the presence of current measurements tends to deteriorate the performance of the state estimator [4]. The third is integrating both measurements considering the different sampling/refresh rates associated with RTU and PMU measurements and corresponding bad data detection and elimination. Fourth is the optimal placement of PMUs within the power system. The integration of PMUs into a power transmission network presents numerous technical benefits, but it comes with high infrastructural costs. For this reason, a tradeoff is necessary. While the cost of PMU devices, associated infrastructure, the cost of upgrading existing substations if not compatible with PMU technology, and the cost of handling big data make it uneconomical to place PMUs in all buses within a power system network, an optimal number of PMUs deployed within the network can improve state estimation in terms of robustness and accuracy [5], [6].

The conventional Optimal Phasor Placement Problem (OPPP) is formulated to determine the minimum number of PMUs required together with their specific locations to make the system completely observable [7]–[10]. Various constraints have been considered in the OPPP, including contingencies such as single or multiple PMU loss and single branch outage. These contingencies are treated as constraints during the formulation of the PMU placement problem. Integration of these constraints results in an increased number of minimum PMUs required for observability and system resiliency as per the results obtained in [11], [12], translating to a higher PMU installation cost.

With the vast deployment of RTU meters in the power system, some applications such as state estimators can greatly benefit from both PMU and RTU measurements. Therefore, the redundant placement of conventional RTU meters would greatly enhance state estimation accuracy, and measurement redundancy and eliminate some of the constraints considered in OPPP, such as PMU loss/outage, while considering PMU measurements only. Furthermore, another challenge associated with integrating RTU and PMU measurements for state estimation is developing an appropriate measurement model to eliminate the nonlinearity associated with RTU measurements in state estimation, such as high computational burden and iterative algorithms. Therefore, a need to develop a robust Linear Hybrid State Estimator (LHSE) arises with the inclusion of RTU measurements in the state estimation model.

II. RELATED STUDIES

Integration of RTU and PMU measurements into HSE has been published in the literature, considering diverse measurement model formulations and PMU placement approaches to enhance state estimation performance. The HSE formulations fall either under two-stage (including both linear and nonlinear) HSE, single-stage nonlinear HSE, or single-stage linear HSE.

In the two-stage HSE, the first stage comprises a nonlinear estimator based on RTU measurements. Power system states obtained from the first stage are improved using a second estimator that uses PMU measurements only [13]–[15]. A modified two-stage HSE meant to address the different refresh rates comprises a nonlinear stage based on RTU and PMU measurements integrated into a nonlinear estimator at the instants when all the measurements are refreshed. A linear estimator is employed when only PMU measurements are refreshed [16]–[19]. For instance, the authors in [20] propose a modified two-stage HSE with the state vector expressed in rectangular coordinates with a sub-optimal number of PMUs employed in the HSE. A nonlinear State Estimator (SE) is used at a time instant when both RTU and PMU measurements are refreshed. A linear state estimator is used for the time instant between two consecutive RTU scans, using pseudo measurements to achieve system observability. In [21], the modified two-stage SE is also proposed for tracking dynamics of a power system states following a fault based on a partial observable network using PMUs. The proposed SE utilizes nonlinear (for RTU and PMU measurements) and linear (for PMU measurements only) estimators. The authors in [22] propose a multi-time interval HSE, subdivided into a steady, quasi-steady, and fluctuant area. The HSE formulation is based on a fusion of parallel estimators (linear and nonlinear) for each area to produce the final estimate. The authors in [23] also proposed a nonlinear SE processing both RTU and PMU measurements when both sets are refreshed and a robust linear SE based on LAV processing PMU measurements at their refresh instants. A limited number of PMUs is considered in the study, with the placement of PMUs assumed to be strategically important. The main challenge associated with these two-stage HSE is using nonlinear algorithms resulting in computational burden and the need for an extra stage for bad data processing.

The single-stage nonlinear HSE combines RTU and PMU measurements into a single nonlinear estimator [24], [25]. In [26], RTU and PMU measurements are integrated into a single-stage nonlinear HSE, with the current phasor measurements related to power system states via constraints. The PMU placement implemented is based on converting critical measurements to redundant measurements yielding partial system observability using PMUs. The authors in [27] also developed a single-stage nonlinear HSE and further analyzed the HSE performance with the PMU current phasor

measurement formulated in rectangular or polar coordinates. Incremental PMU placement is considered using various case studies, with partial and complete system observability via PMUs. A single-stage nonlinear HSE is also proposed in [28], with the PMU current phasors formulated in rectangular coordinates and the state vectors in polar form. The developed HSE utilizes a different number of PMUs, with better results obtained when more PMUs are utilized. The authors in [29] develop a single-stage nonlinear HSE to track power system dynamics while addressing bad data detection using a robust state estimator based on a weight assignment function. This category of HSE is faced with various challenges, such as addressing different measurement refresh rates, bad data processing, and the use of a nonlinear estimation algorithm.

The nonlinearity challenges mentioned previously can be addressed using a single-stage Linear Hybrid State Estimator (LHSE). The single-stage LHSE integrates RTU and PMU measurements into a single linear estimator. The main challenge is the inclusion of RTU measurements into the measurement vector to obtain a linear relationship between the measurement vector and the power system states. Based on recent studies, various methods of including RTU measurements into the measurement vector have been proposed. The authors in [30] developed a linear HSE based on complex linear equations that use a redundant voltage phase angle vector. The formulation is based on the general pi model for transmission lines and transformers. The state estimation algorithm employs the least absolute value algorithm to eliminate the need for a separate bad data processing stage. This linear formulation is extended in [31] using IRLS and M-estimator to address bad data detection. The authors in [32] formulate a linear HSE using an equivalent circuit formulation, an approach that describes the power system in terms of voltage and current variables in rectangular coordinates. Linear circuit models for RTU measurements are developed using equivalent split-circuit representation. Authors in [33] leverage the equivalent circuit formulation approach to establish an entirely linear HSE by reformulating the RTU measurement circuit models based on the circuit analysis principles. The developed HSE model is evaluated based on the Weighted Least Squares (WLS) method and the largest normalized residue for bad data processing.

Various optimization techniques have been proposed for the OPPP using mathematical and metaheuristic algorithms. Mathematical algorithms include Integer linear programming [34]–[37] and exhaustive search [38], [39], while metaheuristic algorithms include Genetic Algorithms, Differential Evolution, Particle Swarm Optimization, and Artificial Bee Colony (ABC). A review by [40] indicates potential research areas for the OPPP since different solutions produce the same number of PMUs at different locations. Mathematical algorithms direct to only one solution while more than one solution may be present. Metaheuristic algorithms can give various solutions, which can be evaluated for the best outcome depending on system constraints. A common evaluation criterion is observability indices such as System Observability Redundant Index (SORI) and Bus Observability Index (BOI). The optimal solution with the highest SORI index is the best set.

The PMU inclusion in the previous studies is based on a limited number of PMUs to evaluate the HSE performance. This work considers existing RTU measurements integrated with optimally placed PMUs to achieve power system observability and resilience against measurement loss. Therefore, this paper proposes an LHSE that can simultaneously handle RTU and PMU measurements. RTU measurements are transformed to current measurements and based on Kirchhoff's Current Law (KCL), a linear measurement model is developed. The proposed state estimator uses real and imaginary voltages as the state variables, later converted to phasor form to obtain estimated voltage magnitude and phase angle. The PMU measurements are utilized in their rectangular form (real and imaginary values). The estimator employs the Weighted Least Absolute Value (WLAV) criterion, a robust method for linear state estimators. The RTU measurements employed in the estimator are randomly distributed within a transmission network representing a system with existing RTU meters. PMU measurements are optimally placed based on the ABC algorithm. The accuracy of the proposed estimator is evaluated based on voltage magnitude error, absolute angle error, and Normalized Cumulative Error (NCE) performance index [41]. The proposed estimator is tested on three standard transmission systems (IEEE 14-Bus, 30-Bus, and 57-Bus).

The main contributions of this paper are:

i. A fully linear measurement model for the proposed LHSE is developed. The formulation is based on modeling a transmission line using voltage and current state variables in rectangular coordinates. The RTU and PMU measurements are further integrated into the LHSE using the voltage and current state variables. The developed LHSE model integrates randomly existing RTU devices and optimally placed PMU devices. The proposed estimator can run on a linear programming solver with no iterative procedure.
ii. The proposed LHSE model can process measurements from RTU meters separately, PMU meters, or hybrid RTU/PMU meters. It is anchored on an existing SCADA system fully observable with RTU meters. The PMUs integrated into the LHSE model are also optimally placed based on SORI and measurement redundancy, guaranteeing observability in either of the scenarios. The proposed approach also guarantees the system monitoring reliability against PMU failure by utilizing hybrid measurements instead of working with PMU measurements only, as in existing studies. The evaluation of the proposed LHSE validates the proposed approach.
iii. An algorithm for the proposed LHSE is developed to make it robust against bad data using WLAV. With the

estimator model being linear, the computational burden due to the use of WLAV is also addressed.

The rest of the paper is organized as follows; Section III gives a methodology for mathematical formulation of proposed LHSE, PMU placement, description of existing RTU measurements considered, and simulation setup description. Section IV gives results and discussion with a conclusion drawn in Section V.

III. METHODOLOGY

The methodology describes the formulation of the proposed LHSE, optimal PMU placement using the ABC algorithm, a description of existing RTU measurements employed in this study, and a simulation description for the state estimation process.

A. PROPOSED LINEAR HYBRID STATE ESTIMATOR (LHSE)

The proposed LHSE mathematical model formulation integrates the use of both RTU and PMU measurements. The power system states in this paper are modeled in a rectangular format comprising real and imaginary bus voltages. RTU measurements conventionally have a nonlinear relationship with system states; hence to develop a linear relationship, the RTU measurements are transformed into equivalent current measurements based on equation (1).

$$I^* = \frac{P + jQ}{V} \tag{1}$$

Given a transmission line connecting buses k and m, the relationship between the current flow (in rectangular form) along the line from either of the buses and the voltage (in rectangular form) at the buses are linked by the branch admittance matrix as shown by equation (2), [42].

$$\begin{bmatrix} i^R_{km} \\ i^I_{km} \\ i^R_{mk} \\ i^I_{mk} \end{bmatrix} = \begin{bmatrix} Y^R_{ff} & Y^R_{ft} & -Y^I_{ff} & -Y^I_{ft} \\ Y^I_{ff} & Y^I_{ft} & Y^R_{ff} & Y^R_{ft} \\ Y^R_{tt} & Y^R_{tf} & -Y^I_{tt} & -Y^I_{tf} \\ Y^I_{tt} & Y^I_{tf} & Y^R_{tt} & Y^R_{tf} \end{bmatrix} \begin{bmatrix} V^R_k \\ V^R_m \\ V^I_k \\ V^I_m \end{bmatrix} \tag{2}$$

The mathematical formulation gives a linear hybrid measurement model shown in equation (3) for the transmission line connecting buses k and m. Based on Kirchhoff's Current Law (KCL), the total current injected at a particular node should be equal to zero. Based on this, the RTU measurements are finally implemented in the measurement model as zero values with the constant components H_{11} up to H_{44} obtained from the application of KCL relating the zero values to power system states. The PMU measurements are also utilized in their rectangular format. The power system state variables, v^R_k, v^R_m, v^I_k and v^I_m are real and imaginary forms of the voltages at buses k and m, respectively. The real and imaginary voltage values measured using PMUs are $v^R_{k,pmu}$, $v^R_{m,pmu}$, $v^I_{k,pmu}$ and $v^I_{m,pmu}$. The real and imaginary current values measured using PMUs are $i^R_{k,pmu}$, $i^R_{m,pmu}$, $i^I_{k,pmu}$ and $i^I_{m,pmu}$. The PMU voltage measurements are related to state variables using a unity matrix, and PMU current measurements are related to state variables using the branch admittance matrix. Finally, e vector represents real and imaginary errors emanating from voltage phasor, current phasor, and RTU measurements. Equation (3) can be summarized as a linear measurement model given in equation (4), where Z represents PMU voltage and current measured values in rectangular form and zero values resulting from the application of KCL for current measurements (obtained from RTU measurements). The H components represent a constant matrix relating Z to power system state variables denoted by x. All the errors arising from both RTU and PMU measurements are denoted by e. The proposed linear measurement model allows system state variables to be determined using a non-iterative state estimation criterion. The system states in this paper are thus obtained using the WLAV criterion method based on linear programming in MATLAB. The WLAV estimation criterion is selected based on its robustness.

$$\begin{bmatrix} v^R_{k,pmu} \\ v^R_{m,pmu} \\ v^I_{k,pmu} \\ v^I_{m,pmu} \\ i^R_{km,pmu} \\ i^I_{km,pmu} \\ i^R_{mk,pmu} \\ i^I_{mk,pmu} \\ 0 \\ 0 \\ 0 \\ 0 \end{bmatrix} = \begin{bmatrix} 1 & 0 & 0 & 0 \\ 0 & 1 & 0 & 0 \\ 0 & 0 & 1 & 0 \\ 0 & 0 & 0 & 1 \\ Y^R_{ff} & Y^R_{ft} & -Y^I_{ff} & -Y^I_{ft} \\ Y^I_{ff} & Y^I_{ft} & Y^R_{ff} & Y^R_{ft} \\ Y^R_{tt} & Y^R_{tf} & -Y^I_{tt} & -Y^I_{tf} \\ Y^I_{tt} & Y^I_{tf} & Y^R_{tt} & Y^R_{tf} \\ H_{11} & H_{12} & H_{13} & H_{14} \\ H_{21} & H_{22} & H_{23} & H_{24} \\ H_{31} & H_{32} & H_{33} & H_{34} \\ H_{41} & H_{42} & H_{43} & H_{44} \end{bmatrix} \times \begin{bmatrix} v^R_k \\ v^R_m \\ v^I_k \\ v^I_m \end{bmatrix} + \begin{bmatrix} e^R_{v,k} \\ e^R_{v,m} \\ e^I_{v,k} \\ e^I_{v,m} \\ e^R_{i,km} \\ e^I_{i,km} \\ e^R_{i,mk} \\ e^I_{i.mk} \\ e^R_k \\ e^R_m \\ e^I_k \\ e^I_m \end{bmatrix} \tag{3}$$

$$\boldsymbol{Z} = \boldsymbol{H}\,\boldsymbol{x} + \boldsymbol{e} \tag{4}$$

The proposed LHSE utilizes PMU and RTU measurements in the same model. The measurements have different refresh rates. To account for this, with the availability of RTU/PMU measurements simultaneously, the estimator provides state estimates based on all the measurements. With the arrival of

RTU measurements only, the linear estimation is based on this type of measurement to produce estimates since the existing RTU measurements are redundant enough to make the entire system observable. With the availability of PMU measurements only, the LHSE depends on these measurements to produce estimates, given that there are optimal PMUs within the system for complete observability. For estimation reliability, in case of system contingency such as PMU loss at the instant of PMU measurement availability, the method proposed in [43] could be applied.

Additionally, at the instant when only RTU measurements are received, the state estimation problem is formulated using a reference bus with the phase angle set to zero since the measurements are not GPS synchronized. With the availability of PMU measurements in the measurement set, the state estimation problem is formulated without using a reference bus, given that PMU measurements are GPS synchronized. To validate the proposed method, state estimation in this paper is solved using two different measurement refresh instances:

i. LHSE model using WLAV with updated RTU/PMU measurements.
ii. LHSE model using WLAV with updated PMU measurements only.

B. OPTIMAL PMU PLACEMENT

The OPPP primarily investigates the minimum number of PMUs required to achieve observability for the entire power system network. A power system is entirely observable if the available measurement infrastructure allows the determination of voltage and phase angle at every bus of the network [44]. A PMU installed at a bus can measure the bus voltage phasor and the current phasor in the branches connected to the considered bus. With the line parameters known, the voltage of the adjacent buses can also be computed. Conventionally, determining the minimum number and specific PMU locations can be formulated as a constrained optimization problem. The objective function minimizes the total number of PMUs to be placed, while the observability of each bus in the network is the constraint. It is possible to get multiple optimal solutions with the same number of PMUs. In this research, Bus Observability Index (BOI) and System Observability Redundancy Index SORI evaluate the quality of the solution. BOI represents the times that a particular bus is observed and is given by the total number of PMUs observing a specific bus. SORI is obtained as a sum of BOI at all buses installed with PMUs in the entire system.

1) PROBLEM FORMULATION CONSIDERING NORMAL CASE

In the normal case, the PMU placement objective is to achieve full system observability without considering any system contingency. The objective function is an optimization problem that minimizes the number of PMUs placed in a system considering observability constraint. The objective function is formulated in equation (5), [2].

$$F = \min \sum_{k=1}^{N} w_k x_k \tag{5}$$

where F is the objective function for OPPP

N refers to the total number of buses in a particular network.

$X = [x_1, \cdots, x_n]$ is a binary decision variable associated with bus k;

$$x_k = \begin{cases} 1 & \text{if a PMU is placed at bus } k \\ 0 & \text{if no PMU is placed a bus } k \end{cases}$$

w_k represents possible weight assigned to the k^{th} bus

The objective function is subject to observability constraint given in equation (6),

$$\boldsymbol{f}(\boldsymbol{X}) \geq \hat{\mathbf{1}} \tag{6}$$

where $f(X)$ is a vector, which depends on the PMUs set, expressing the observability of each node as;

$$\mathrm{f_k} = \begin{cases} 1 & \text{if bus k is observable} \\ 0 & \text{if bus k is unobservable} \end{cases}$$

$\hat{\mathbf{1}}$ is $[1, \cdots, 1]$, an N size vector whose entries are all 1.

The observability constraint of each bus, given by the vector function $f(X)$ of equation (6), is expressed through a set of linear equations derived from matrix multiplication of $A.X$, where A represents a binary connectivity matrix that indicates a connection between buses associated to the topology of a particular power system network, whose entries are given in equation (7).

$$A_{km} = \begin{cases} 1 & \text{if } k = m \\ 1 & \text{if buses } k \text{ and } m \text{ are connected} \\ 0 & \text{if buses } k \text{ and } m \text{ are not connected} \end{cases} \tag{7}$$

For instance, given the IEEE 14-Bus system, the objective function is given in equation (8). The weight assigned to the k^{th} bus in this paper is 1 when finding the optimal number of PMUs, indicating that the cost of deploying PMUs at all the buses is equal.

$$F = \min \sum_{k=1}^{14} x_k \tag{8}$$

The constraint $f(X)$ is derived from IEEE 14 bus connectivity matrix given in equation (9) with the constraints given in equation (10). BOI is derived from the connectivity matrix, provided by the sum of each row with a PMU installed at bus 1 has a BOI of 3, as shown in equation (11). The Sum of BOI for all buses installed with PMUs gives the entire system

SORI as given in equation (12).

$$A = \begin{bmatrix} 1&1&0&0&1&0&0&0&0&0&0&0&0&0 \\ 1&1&1&1&1&0&0&0&0&0&0&0&0&0 \\ 0&1&1&1&0&0&0&0&0&0&0&0&0&0 \\ 0&1&1&1&1&0&1&0&1&0&0&0&0&0 \\ 1&1&0&1&1&1&0&0&0&0&0&0&0&0 \\ 0&0&0&0&1&1&0&0&0&0&1&1&1&0 \\ 0&0&0&1&0&0&1&1&1&0&0&0&0&0 \\ 0&0&0&0&0&0&1&1&0&0&0&0&0&0 \\ 0&0&0&1&0&0&1&0&1&1&0&0&0&1 \\ 0&0&0&0&0&0&0&0&1&1&1&0&0&0 \\ 0&0&0&0&0&0&0&0&1&1&1&0&0&0 \\ 0&0&0&0&0&0&0&0&1&1&1&0&0&0 \\ 0&0&0&0&0&1&0&0&0&0&0&1&1&1 \\ 0&0&0&0&0&0&0&0&1&0&0&0&1&1 \end{bmatrix} \tag{9}$$

$$\begin{aligned} f_1 &= x_1 + x_2 + x_5 \geq 1 \\ f_2 &= x_1 + x_2 + x_3 + x_4 + x_5 \geq 1 \\ f_3 &= x_2 + x_3 + x_4 \geq 1 \\ f_4 &= x_2 + x_3 + x_4 + x_5 + x_7 + x_9 \geq 1 \\ f_5 &= x_1 + x_2 + x_4 + x_5 + x_6 \geq 1 \\ f_6 &= x_5 + x_6 + x_{11} + x_{12} + x_{13} \geq 1 \\ f_7 &= x_4 + x_7 + x_8 + x_9 \geq 1 \\ f_8 &= x_7 + x_8 \geq 1 \\ f_9 &= x_4 + x_7 + x_9 + x_{10} + x_{14} \geq 1 \\ f_{10} &= x_9 + x_{10} + x_{11} \geq 1 \\ f_{11} &= x_6 + x_{10} + x_{11} \geq 1 \\ f_{12} &= x_6 + x_{12} + x_{13} \geq 1 \\ f_{13} &= x_6 + x_{12} + x_{13} + x_{14} \geq 1 \\ f_{14} &= x_9 + x_{13} + x_{14} \geq 1 \end{aligned} \tag{10}$$

$$BOI = \sum_{k=1}^{N} A_k \tag{11}$$

$$SORI = \sum_{k=1}^{N} BOI_k \tag{12}$$

2) PROBLEM FORMULATION CONSIDERING SINGLE PMU FAILURE

For a system installed with PMUs, there is a need to enhance power system monitoring resilience and reliability against PMU failure. If a state estimation depends on PMU measurements only, a single PMU failure is addressed when each bus in the power system is observed by at least two PMUs. The observability constraint given in equation (6) is thus modified where $\hat{1}$ becomes $[2, 2, \cdots, 2]$, an N size vector whose entries are 2. A PMU failure is more severe than other contingencies, such as a single line/branch outage [45]. Therefore, if a bus is observed by two PMUs, a branch loss will not affect the power system observability.

3) OPTIMIZATION ALGORITHM USING ABC

ABC optimization algorithm is employed to find optimal PMU locations for the OPPP with its efficiency and excellent exploration depicted in existing studies [10], [46]. It is a metaheuristic algorithm proposed in [47] and inspired by the intelligent behavior of bee swarms. The algorithm has been applied in solving several optimization problems, mostly in engineering, because of its robustness and ease of implementation [48]. The bee swarms are categorized into three groups, employed bees, onlooker bees, and scout bees.

The role of employed bees is to explore nectar (food) sources and pass the information about the nectar amount to onlooker bees. If an employed or onlooker bee exhausts a food source, the corresponding bee will play the role of a scout bee to search randomly to get out of a local trap. Once a scout bee finds a solution, it becomes an employed bee. Thus, the ABC algorithm comprises four sequential phases: initialization, employed bee phase, onlooker bee, and scout bee phase [49]. ABC algorithm has been applied in solving the OPPP in various studies [10], [46]. The initialization phase involves the definition of ABC parameters that include colony size, number of food sources (N_p), system size, limit for scout bee to take over, and maximum iterations. System information such as objective function and constraints are also initialized at this phase. Food sources (F_j^i) represent a possible solution for PMU placement which is randomly generated using equation (13). Where $i = 1, 2, \cdots N_p$, $j = 1, 2, \cdots D$, with D being a randomly generated D dimensional vector.

$$F_j^i = F_j^{min} + rand(F_j^{max} - F_j^{min}) \tag{13}$$

The employed bee phase explores new solutions representing new PMU locations using equation (14), with k not equal to i. ψ_j^i is a randomly generated number between -1 and 1.

$$F_{ij}^{new} = F_j^i + \psi_j^i(F_j^i - F_j^k) \tag{14}$$

Next, the fitness value fv_i of the generated PMU locations is obtained using equation (15). Consequently, the best solutions are used to update new PMU locations.

$$fv_i = \begin{Bmatrix} \dfrac{1}{1+f_i} & f_i \geq 0 \\ 1 + |f_i| & f_i < 0 \end{Bmatrix} \tag{15}$$

The onlooker bee phase selects a solution based on a probability P_i given by equation (16). The selected solution undergoes employed bee phase steps to generate a new solution.

$$P_i = \frac{fv_i}{\sum_{n=1}^{N_p} fv_n} \tag{16}$$

After a search reaches a set limit without achieving a better solution, the search randomly moves to a scout bee phase to find a new solution based on equation (13). The search process for optimal PMU locations undergoes all the phases until all conditions are met, giving an output consisting of the minimum optimal number and specific PMU locations.

TABLE 1. Existing RTU measurement configuration.

Measurement Type	IEEE 14 BUS	IEEE 30 BUS	IEEE 57 BUS
Voltage magnitude	5	14	28
Real power injection	9	16	34
Reactive power injection	9	16	34
Real power flow from a bus	11	25	50
Reactive power flow from a bus	11	25	50
Real power flow to a bus	6	16	32
Reactive power flow to a bus	6	16	32
Total measurements (m)	57	128	260
Number of states to be estimated (n)	28	60	114
Redundancy (m/n)	2.04	2.13	2.28

C. EXISTING SCADA-BASED RTU MEASUREMENTS

In the proposed LHSE, the power system is assumed to have existing SCADA-based RTU meters enough to make the system observable. The RTU measurements considered comprise voltage magnitude, real and reactive power injection, and real and reactive power flow from/to a bus. The RTU measurements are given in table 1, where the various measurements are assumed to be randomly distributed within the system to achieve a measurement redundancy greater than 1.

In a particular power system, the number of branches is usually higher than the number of buses; thus, the number of voltage magnitudes measurements and power injection is less than corresponding power flow measurements. From the measurements assumed, the redundancy of IEEE 14 bus, IEEE 30 bus, and IEEE 57 bus is 2.04, 2.13, and 2.28, respectively. The specific RTU measurement locations are randomly determined in MATLAB using the randperm function. The specific locations for the three test cases are given in table 2. For instance, the five voltage magnitude measurement locations for IEEE 30 bus are located at buses 1, 3, 4, 11, and 13, while the 14-voltage magnitude measurement locations for IEEE 30 buses are located at buses 1, 3, 4, 5, 8, 10, 12, 18, 21, 24, 25, 26, 28, and 29.

D. SIMULATION DESCRIPTION

The simulations are performed in MATLAB2019a using MATPOWER with the test case data available online by MATPOWER 7.0. The MATLAB is implemented on a 8 GB RAM, Intel(R) Core (TM) i7-8565U CPU @ 1.80GHz 1.99 GHz, processor. The optimal PMU placement locations are determined through simulation using system data for each test case and ABC algorithm. The ABC algorithm parameter settings are shown in table 3. The basic ABC algorithm flow chart is given in figure 1. The algorithm's output comprises

TABLE 2. RTU measurement locations for three test cases.

Measurement Type	**IEE 14 BUS**	**IEEE 30 BUS**	**IEEE 57 BUS**
Voltage Magnitude	1, 3, 4, 11, 13	1, 3, 4, 5, 8, 10, 12, 18, 21, 24, 25, 26, 28, 29	1, 2, 6, 8, 9, 13, 21, 22, 23, 27, 30, 31, 35, 37, 39, 40, 41, 42, 43, 44, 45, 47, 49, 50, 51, 55, 56, 57
Real/Reactive power injection	1, 2, 3, 6, 7, 9, 10, 12, 13	1, 2, 4, 5, 7,9,10,14,15, 16,18, 19, 21, 24, 29, 30	1, 3, 4, 5, 6, 8, 9, 12, 13, 15, 16, 18, 19, 20, 21, 24, 25, 26, 30, 31, 32, 33, 35, 40, 41, 43, 48, 49, 51, 52, 53, 55, 56, 57
Real/Reactive power flow from a bus	1, 2, 3, 6, 8, 11, 13, 14, 17, 19, 20	2, 3, 5, 7, 8, 9, 10, 11, 12, 13, 16, 17, 19, 20, 22, 23, 26, 31, 32, 33, 34, 35, 36, 38, 39	1, 2, 4, 5, 7, 8, 10, 14 16, 17, 19, 20, 21, 22, 23 24, 26, 27, 28, 29, 30, 31 32, 33, 34, 36, 37, 38, 39, 41, 42, 43, 45, 46, 47 49, 52, 54, 55, 57, 58 59, 62, 64, 67, 69, 76, 77, 79, 80
Real/Reactive power flow to a bus	1, 3, 7, 11, 14, 19	1, 4, 6, 14, 15, 18, 24, 25,27, 29, 30, 31, 32, 36, 39, 40	2, 9, 15, 18, 23, 24, 25, 27, 29, 30, 31, 35, 36, 40, 43, 44, 45, 48, 49, 50, 54, 55, 56, 57, 65, 67, 70, 72, 74, 77, 78, 80

TABLE 3. ABC algorithm parameter settings.

System size	IEEE 14-bus	IEEE30-bus	IEEE 57-bus
Colony size	200	250	300
Food sources	100	125	150
Limit	100	100	100
Maximum iterations	500	500	500

different OPPP solutions with specific PMU locations, corresponding SORI, and bus redundancy for a particular solution.

The proposed hybrid state estimation utilizing RTUs and optimally placed PMUs is done using the following steps;

Step 1: Input test case data

Step 2: Find optimal PMU locations using the ABC algorithm

Step 3: Find RTU locations randomly

Step 4: Perform load flow calculation and store the results (voltage magnitude, phase angle, real/reactive power injection, real/reactive power flow). The voltage magnitude and phase angle are used as reference values in state estimation.

Step 5: Extract PMU and RTU measurements from load flow results

Step 6: Model mathematically accuracy of measurement meters as noise which is induced into the PMU and RTU measurements using equation (17),

$$z = (\sigma * randn\,(1) + A) \tag{17}$$

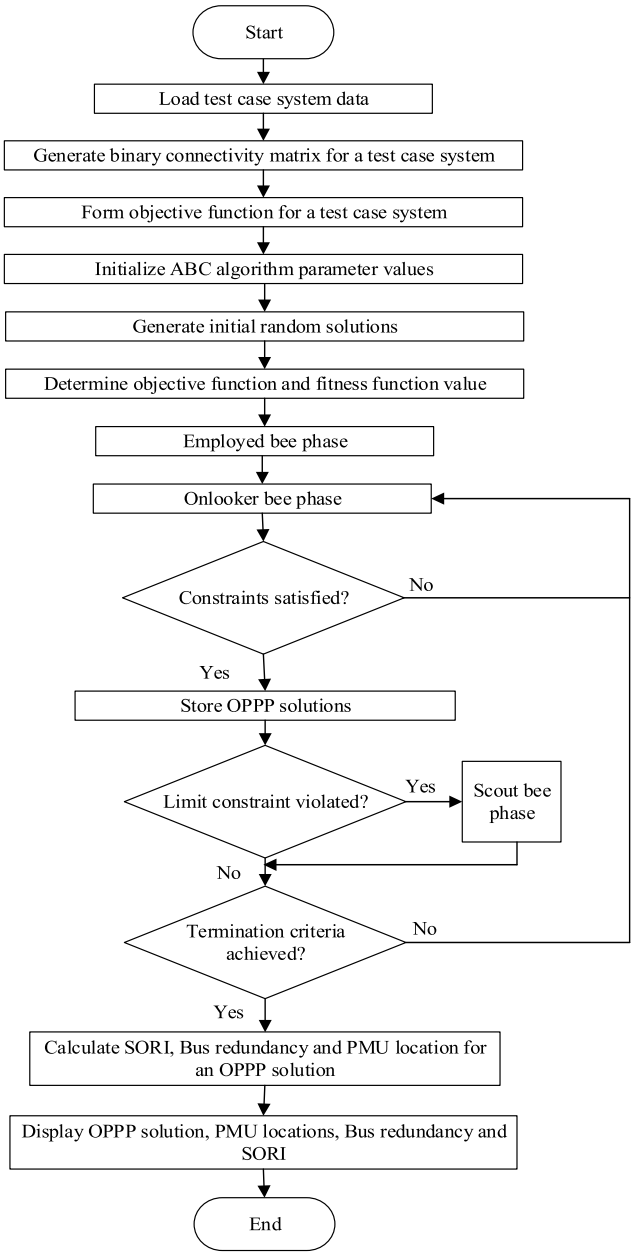

FIGURE 1. ABC algorithm flow chart.

where Z is the new value for PMU and RTU measurements after adding noise, σ is the standard deviation associated with various measurements as given in table 4, obtained from [50]. The term *randn(1)* is a random number with zero mean and normal distribution varying between -1 and 1. The Load flow value for a particular measurement is given by A.

Step 7: Store the new measurement sets (with noise added) for PMU and RTU measurements.

Step 8: Generate the proposed LHSE measurement model using new PMU and RTU measurements.

Step 9: Run state estimation for different cases under evaluation, as shown in table 5.

TABLE 4. The standard deviation used for various RTU and PMU measurements.

Measurement Type	Standard Deviation
Voltage magnitude	0.01
Real power injection	0.02
Reactive power injection	0.04
Real power flow	0.02
Reactive power flow	0.04
Voltage phasor	0.001
Current phasor	0.001

TABLE 5. The different cases under evaluation for the proposed LHSE.

Case	Description
Case 1	Evaluation of proposed LHSE considering the normal operation
Case 2	Evaluation of proposed LHSE considering single PMU loss
Case 3	Evaluation of the proposed LHSE considering bad data existence

Step 10: Output the state estimation results, voltage magnitude, phase angle errors, and NCE values considering the different cases. The NCE value is calculated using equation (18), where n is the number of buses per test case.

$$NCE = \frac{1}{2n}\left(\sum_{i=1}^{2n} |Actual\ value_i - Estimated\ value_i|\right) \quad (18)$$

IV. RESULTS AND DISCUSSION

This section presents the results obtained from optimal PMU placement and discusses the selection of a particular solution. State estimation is performed considering three different cases; first, the availability of all optimal PMU measurements is referred to as PMU normal operation. Secondly, state estimation considers single PMU loss with all measurements from a single PMU not available for state estimation due to a PMU failure contingency. Finally, the robustness of the proposed LHSE considering bad data is also presented.

A. OPTIMAL PMU PLACEMENT CONSIDERING NORMAL CASE

The optimal PMU placement locations are obtained based on the ABC algorithm. The results obtained consider the normal state of the power system without including either contingencies or zero injection buses. It also considers a PMU with enough channels for connection to transmission lines. Five different placement solutions for IEEE 14-bus are shown in table 6.

All the solutions obtained require a minimum of four PMUs to be placed in the IEEE 14 bus system for complete observability. The solutions are given alongside respective BOI for a particular PMU solution showing the number of times the available PMUs observe a bus within a given solution. The optimal PMU placement solution selected for

TABLE 6. IEEE 14-bus different placement solutions.

PMU locations	Bus number	**2 6 7 9**	2 6 8 9	2 7 11 13	2 7 10 13	2 8 10 13
BOI (Number of times the PMU set observes a bus)	1	**1**	1	1	1	1
	2	**1**	1	1	1	1
	3	**1**	1	1	1	1
	4	**3**	2	2	2	1
	5	**2**	2	1	1	1
	6	**1**	1	2	1	1
	7	**2**	2	1	1	1
	8	**1**	1	1	1	1
	9	**2**	1	1	2	1
	10	**1**	1	1	1	1
	11	**1**	1	1	1	1
	12	**1**	1	1	1	1
	13	**1**	1	1	1	1
	14	**1**	1	1	1	1
SORI		**19**	17	16	16	14
Bus redundancy		**4**	3	2	2	0
Average computational time		1.992s				

this test case comprises PMU locations at buses 2, 6, 7, and 9, given that it has the highest SORI of 19 and also a bus redundancy of 4 with buses 4, 5, 7, and 9 being observed by more than one PMU. Bus redundancy in this context means the total number of buses observed more than once by a particular PMU solution.

For the IEEE 30-bus system, nine different placement solutions are obtained, as shown in table 7. The minimum number of PMUs required for complete observability is ten for all solutions obtained. The solution with the highest SORI of 50 and bus redundancy of 14 is selected as the optimal set with the PMU locations at buses 1, 2, 6, 9, 10, 12, 15, 19, 25, and 27. With this PMU set, the redundant buses are 1, 2, 4, 6, 9, 10, 12, 14, 15, 18, 20, 25, 27, and 28.

Table 8 shows four different solutions obtained for the IEEE 57-bus test case with a minimum of 17 PMUs required for the complete system observability. The optimal PMU set selected comprises PMU locations at buses 1, 4, 6, 9, 15, 20, 24, 28, 31, 32, 36, 38, 39, 41, 47, 50, and 53 with a SORI of 72 and bus redundancy of 14. The buses observed more than once by the PMU set are 1, 3, 4, 5, 6, 8, 11, 13, 15, 31, 32, 37, 48, and 49.

To validate the ABC algorithm under normal operation, a comparison between the placement solutions obtained using the proposed ABC algorithm in this research with other existing ABC studies is given in table 9. The results indicate that

TABLE 7. IEEE 30-bus different placement solutions.

Minimum Number of PMUs	PMU locations	SORI	Bus redundancy	Redundant buses
10	**1 2 6 9 10 12 15 19 25 27**	**50**	**14**	**1 2 4 6 9 10 12 14 15 18 20 25 27 28**
10	2 3 6 9 10 12 15 20 25 27	50	13	1 2 4 6 9 10 12 14 15 20 25 27 28
10	2 4 6 10 11 12 15 19 25 27	50	13	2 4 6 9 10 12 14 15 18 20 25 27 28
10	2 4 6 10 11 12 15 18 25 27	50	12	2 4 6 9 10 12 14 15 18 25 27 28
10	2 3 6 9 10 12 18 24 25 27	49	12	1 2 4 6 9 10 15 22 24 25 27 28
10	1 6 7 9 10 12 15 19 25 27	48	14	2 4 6 7 9 10 12 14 15 18 20 25 27 28
10	3 5 6 9 10 12 15 18 25 27	48	13	2 4 6 7 9 10 12 14 15 18 25 27 28
10	1 2 6 9 10 12 19 23 25 27	48	12	1 2 4 6 9 10 15 20 24 25 27 28
10	3 6 7 9 10 12 15 18 25 27	48	12	4 6 7 9 10 12 14 15 18 25 27 28
Average Computational time	3.225s			

the minimum number of PMUs obtained is 4, 10, and 17 for the three test cases. The computation time obtained varies based on the computational environment employed.

A comparison of the minimum number of PMUs obtained using the ABC algorithm with that of different algorithms in the literature is shown in table 10. For IEEE 14-bus systems, a minimum of 4 PMUs are required for complete observability. For IEEE 30-bus and IEEE 57-bus, a minimum of 10 and 17 PMUs have been obtained using other algorithms. The variation observed is based on the SORI value despite presenting an equal optimal number of PMUs.

B. OPTIMAL PMU PLACEMENT CONSIDERING SINGLE PMU LOSS

For a system based on PMU devices only, the solutions given in table 11 were obtained for the PMU placement considering a single PMU failure in the problem formulation. IEEE 14-bus, 30-bus, and 57-bus require a minimum

TABLE 8. IEEE 57-bus different placement solutions.

Minimum Number of PMUs	PMU locations	SORI	Bus redundancy	Redundant buses
17	**1 4 6 9 15 20 24 28 31 32 36 38 39 41 47 50 53**	**72**	**14**	**1 3 4 5 6 8 11 13 15 31 32 37 48 49**
17	1 4 7 9 15 20 22 25 27 32 36 38 41 47 51 53 57	71	14	1 3 6 8 10 11 13 15 21 22 37 38 48 56
17	1 6 7 9 15 19 22 25 27 32 36 38 41 46 51 53 57	71	13	1 6 7 8 10 11 13 14 15 22 37 38 56
17	1 4 9 13 20 22 25 27 29 32 36 41 45 47 51 53 57	69	10	9 10 11 12 13 15 21 28 52 56
Average time	6.530s			

TABLE 9. The comparison of obtained results with the ABC algorithm in other studies.

	Test case	IEEE 14-BUS	IEEE 30-BUS	IEEE 57-BUS
Obtained Results	PMUs	4	10	17
	SORI	19	50	72
	Time(Seconds)	1.992	3.225	6.530
ABC [10]	PMUs	4	10	-
	SORI	19	50	-
	Time(Seconds)	7.439	14.775	-
ABC [46]	PMUs	4	10	17
	SORI	19	50	72
	Time(Seconds)	40	-	-

of 9, 21, and 33 PMUs, respectively, for the system to be resilient against a single PMU failure. The results obtained show that for a system depending on PMUs only, shielding the system against PMU loss increases the cost. The number of PMUs required under a normal case needs to be increased to improve system reliability. For instance, the number of PMUs for the IEEE 14-bus rises from 4 to 9, while that of the IEEE 57-bus increases from 17 to 33.

In this work, the optimal number of PMUs under the normal case is integrated with existing RTU devices to achieve the same reliability and resilience against single PMU loss.

C. EVALUATION OF THE PROPOSED LHSE CONSIDERING THE NORMAL OPERATION

With optimal PMU locations identified, the respective measurements are integrated with RTU measurements for the proposed estimator. The proposed LHSE is evaluated based on individual estimated states (voltage and phase angle) errors and the NCE performance index. The difference between the reference values (based on load flow results) and estimated values for all system buses give the errors. The simulation results are shown in figures 2 to 7. For all three test cases, state estimation based on PMU/RTU measurements presents less estimation error for both voltage magnitude and absolute phase angle for most system buses.

TABLE 10. Comparison of obtained results with that of other OPPP algorithms.

	Test case					
Search method	IEEE 14-bus		IEEE 30-bus		IEEE 57-bus	
	PMUs	SORI	PMUs	SORI	PMUs	SORI
Proposed ABC	**4**	**19**	**10**	**50**	**17**	**72**
BPSO [51]	4	19	10	48	-	-
ILP [52]	4	-	10	-	-	-
TLBO [53]	4	19	10	46	17	66
Firefly [54]	4	19	10	50	17	72
GWO [55]	4	19	10	52	17	71

For further performance evaluation, NCE values indicating the estimation accuracy based on various measurements are shown in table 12. A lower NCE value indicates higher estimation accuracy. For the three test cases, state estimation based on the combination of PMU and RTU measurements records a lower NCE value than estimation based on PMU measurements. As the system size increases, the NCE values also increase; this may be attributed to the number of buses adding to individual estimated value errors. The computational time for the state estimation process is given in table 13. The estimation based on PMU/RTU measurements requires almost equal estimation time as the use of PMU measurements only.

D. EVALUATION OF THE PROPOSED LHSE CONSIDERING SINGLE PMU LOSS

Evaluation of the proposed LHSE involves initiating a single PMU loss for the three test cases. A single PMU loss means the absence of all measurements from one PMU due to a contingency such as PMU failure. The single PMU loss is randomly initiated in each test case to indicate unpredictability in PMU failure. For the IEEE 14-bus test case, the optimal PMU locations considered, as shown in table 5, are 2, 6, 7, and 9. PMU loss may be initiated at either of the four PMU locations and for IEEE 14 bus, a PMU loss is initiated at bus 6. Therefore, the voltage phasor at bus six and the current phasors for the connected transmission lines are no longer used in state estimation. The estimator's performance in terms of voltage magnitude error and absolute angle error is given in figures 8 and 9, respectively. The estimation error is high for buses 6, 11, 12, and 13 for both voltage and phase angle when using PMU measurements only.

To further examine the performance of the IEEE 14 bus, the reference values are compared with estimated values. Considering single PMU loss at bus 6, figures 10 and 11

TABLE 11. Optimal solutions considering single PMU loss for a system based on PMU measurements only.

Test System	Minimum number of PMUS	PMU locations	SORI	Computational time
IEEE 14-bus	9	2, 4, 5, 6, 7, 8, 9,11, 13	39	2.357s
		1, 2, 3, 6, 7, 8, 9, 10, 13	34	
IEEE 30-bus	21	1, 2, 3, 5, 6, 9, 10, 11, 12, 13, 15, 17, 18, 20, 22, 24, 25, 26, 27, 28, 29	83	3.450s
		1, 3, 5, 7, 8, 9, 10, 11, 12, 13, 15, 16, 19, 20, 21, 23, 25, 26, 28, 29, 30	72	
IEEE 57-bus	33	1, 3, 4, 6, 9, 11, 12, 15, 19, 20, 22, 24, 25, 27, 28, 29, 30, 32, 33, 35, 36, 38, 39, 41, 45, 46, 47, 50, 51, 53, 54, 56, 57	129	7.216s
		1, 2, 4, 6, 9, 12, 15, 19, 20, 22, 24, 25, 27, 28, 29, 31, 32, 33, 34, 36, 37, 38, 41, 43, 45, 46, 47, 50, 51, 53, 54, 56, 57	127	

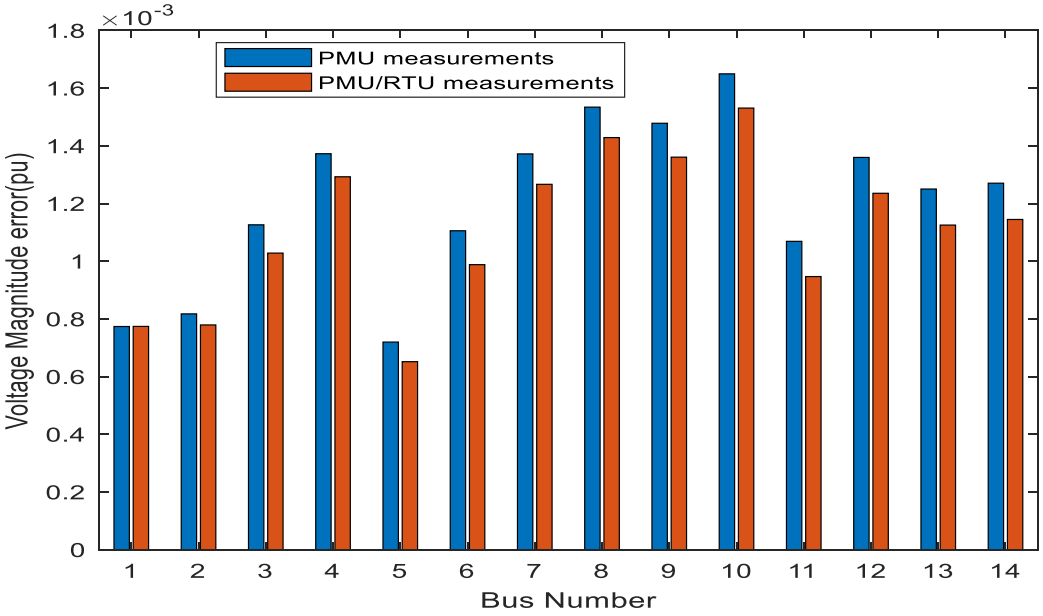

FIGURE 2. Voltage magnitude error for IEEE 14-bus.

TABLE 12. NCE values considering normal system operation.

System	PMU/RTU measurements	PMU measurements
IEEE 14 BUS	$\mathbf{0.51 \times 10^{-2}}$	$\mathbf{1.13 \times 10^{-2}}$
IEEE 30 BUS	$\mathbf{0.87 \times 10^{-2}}$	$\mathbf{1.44 \times 10^{-2}}$
IEEE 57 BUS	$\mathbf{1.64 \times 10^{-2}}$	$\mathbf{2.10 \times 10^{-2}}$

TABLE 13. State estimation computational time considering normal system operation.

System	PMU/RTU measurements	PMU measurements
IEEE 14 BUS	0.002291 s	0.002246 s
IEEE 30 BUS	0.003338 s	0.003147 s
IEEE 57 BUS	0.006323 s	0.005613 s

show voltage magnitude and absolute phase angle for reference values based on load flow, estimated values based on PMU measurements only, and estimated values based on PMU/RTU measurements. It is shown that there are no estimated values at buses 6, 11, 12, and 13 for both voltage and phase angle when using PMU measurements only. The error obtained at the said buses is thus attributed to estimation failure at the specific buses due to unobservability. For the estimator utilizing both PMU and RTU measurements, voltage magnitude and phase angle estimates for all the buses are obtained.

The performance is further illustrated in table 14, showing the actual estimated values for IEEE 14-bus considering PMU loss at bus 6. Zero values for four buses (6, 11, 12, 13) indicate estimation failure at the buses. The estimation failure for the

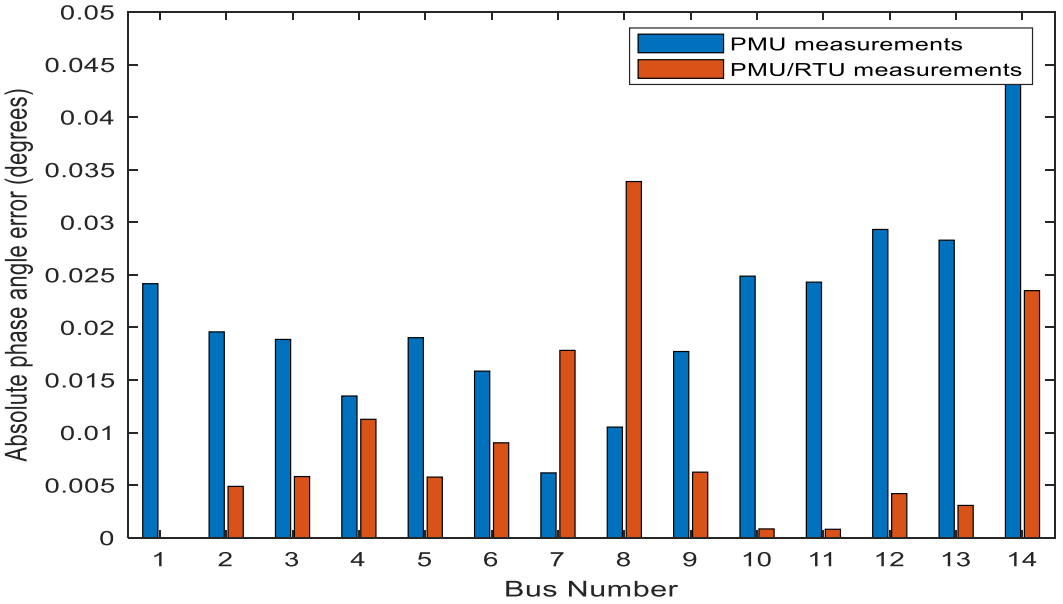

FIGURE 3. Absolute phase angle error for IEEE 14-bus.

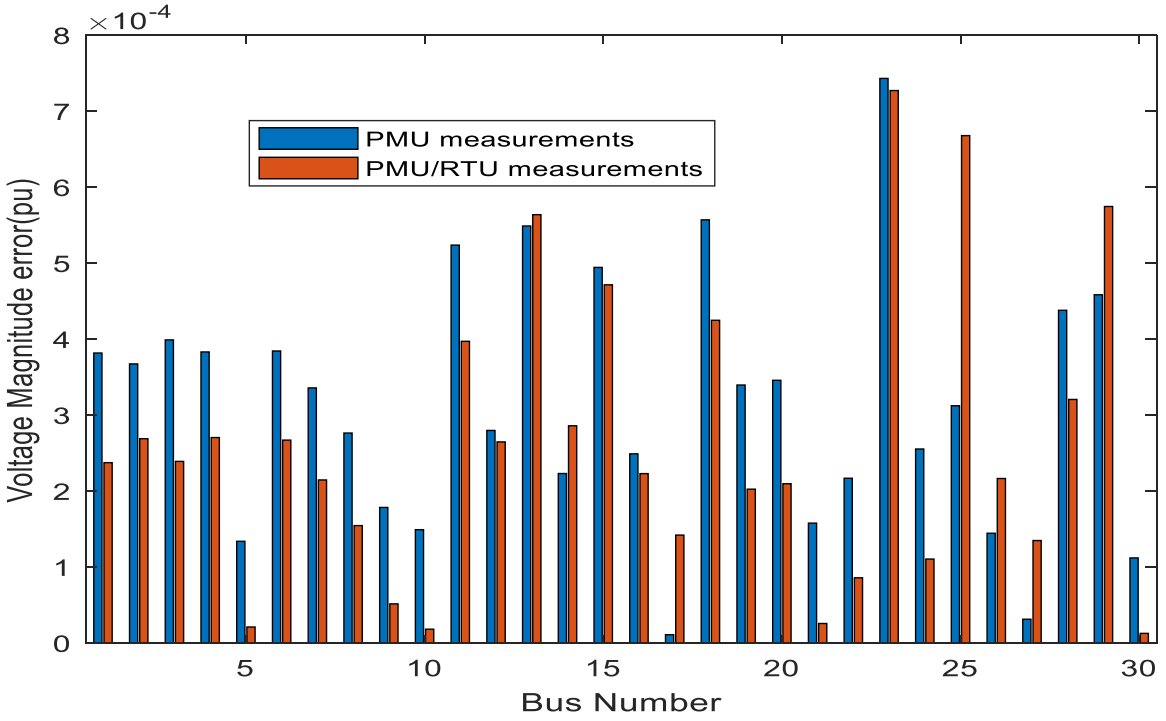

FIGURE 4. Voltage magnitude error for IEEE 30-bus.

case of PMU measurements only could be explained using the IEEE 14-bus topology shown in figure 12. The buses in red indicate PMU placement on such buses. Buses directly connected to the red buses are observable, indicating that their voltage phasors can be calculated based on the PMU readings. Therefore, bus six is directly connected to buses 5, 11, 12, and 13; a failure in PMU placed at bus six renders buses 6, 11, 12, and 13 unobservable, resulting in estimation failure. Bus 5 is a redundant bus observed by two PMUs placed at buses 6 and 2, and consequently, with PMU failure at bus 6, its state can still be estimated relying on PMU at bus 2. Hybrid estimation based on PMU and RTU measurements is not affected by PMU loss at bus six, even with the RTU measurements randomly distributed.

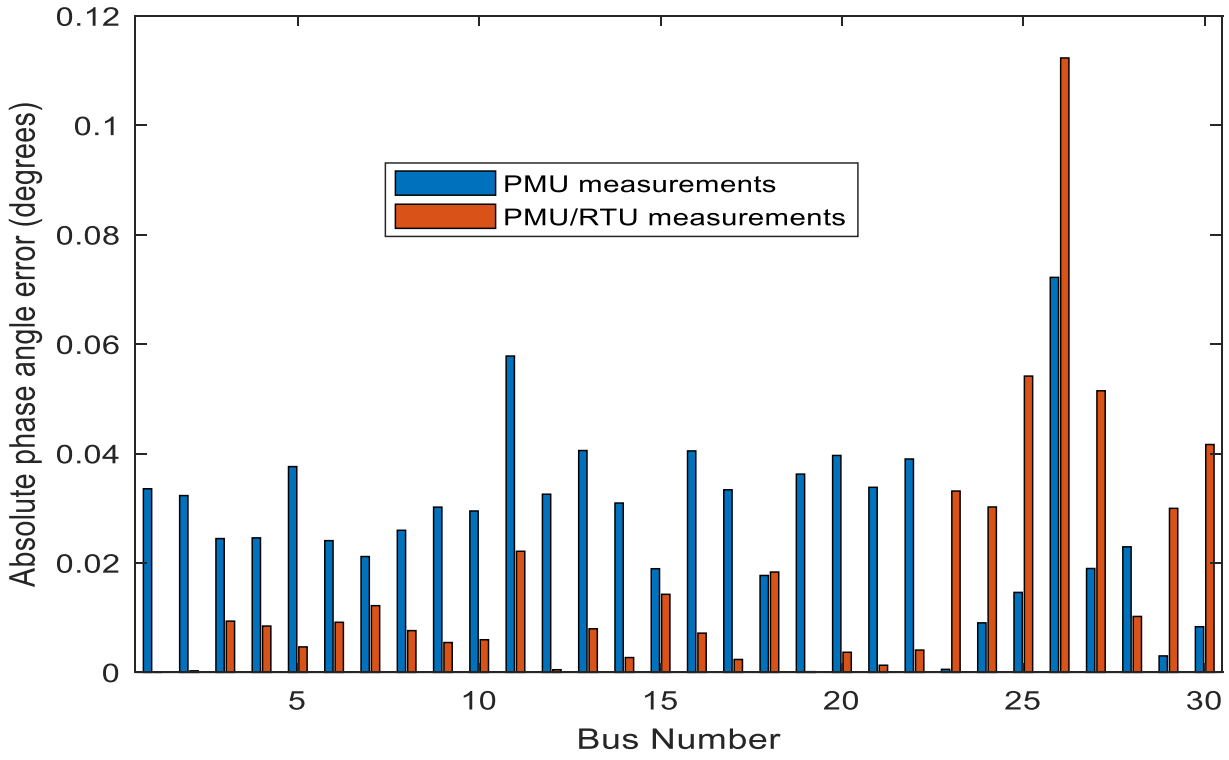

FIGURE 5. Absolute phase angle error for IEEE 30-bus.

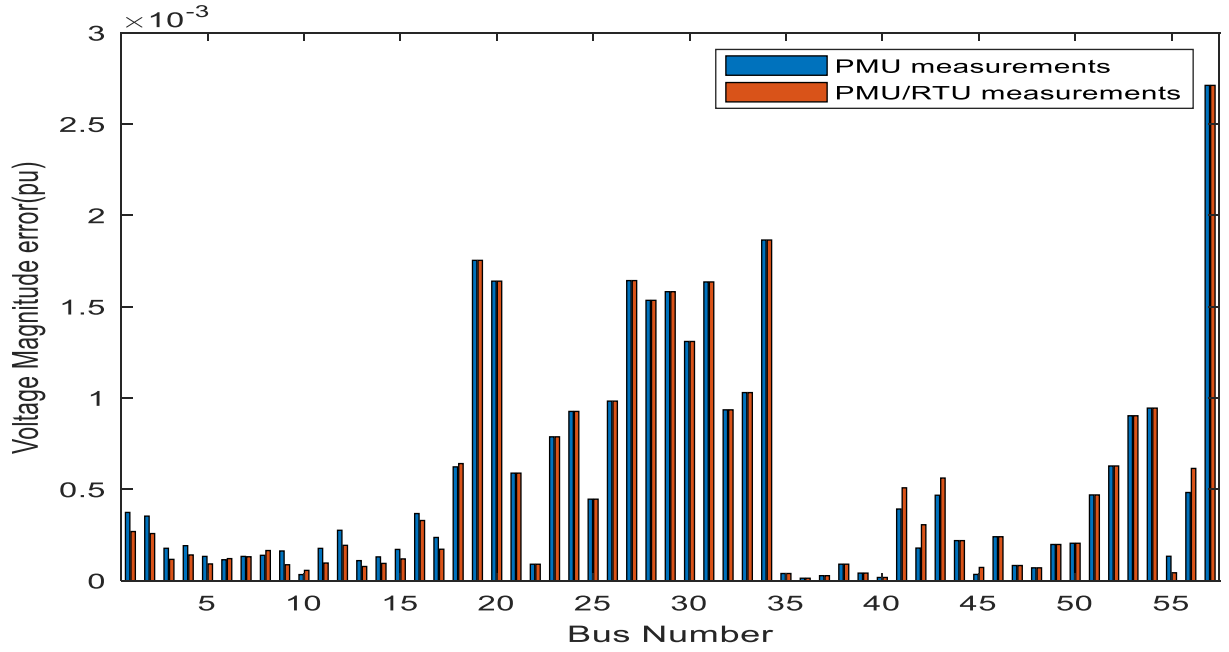

FIGURE 6. Voltage magnitude error for IEEE 57-bus.

For IEEE 30-bus test case shown in figure 13, ten PMUs are placed at buses 1, 2, 6, 9, 10, 12, 15, 19, 25, and 27, as shown in figure 13. A single PMU loss is initiated randomly at bus 10. The voltage magnitude error and absolute phase angle error are shown in figures 14 and 15, respectively. With a single PMU loss at bus 10 for the IEEE 30-bus system, state estimation based on PMU measurements fails for buses 17, 21, and 22, as indicated by both voltage and phase angle error at the respective buses.

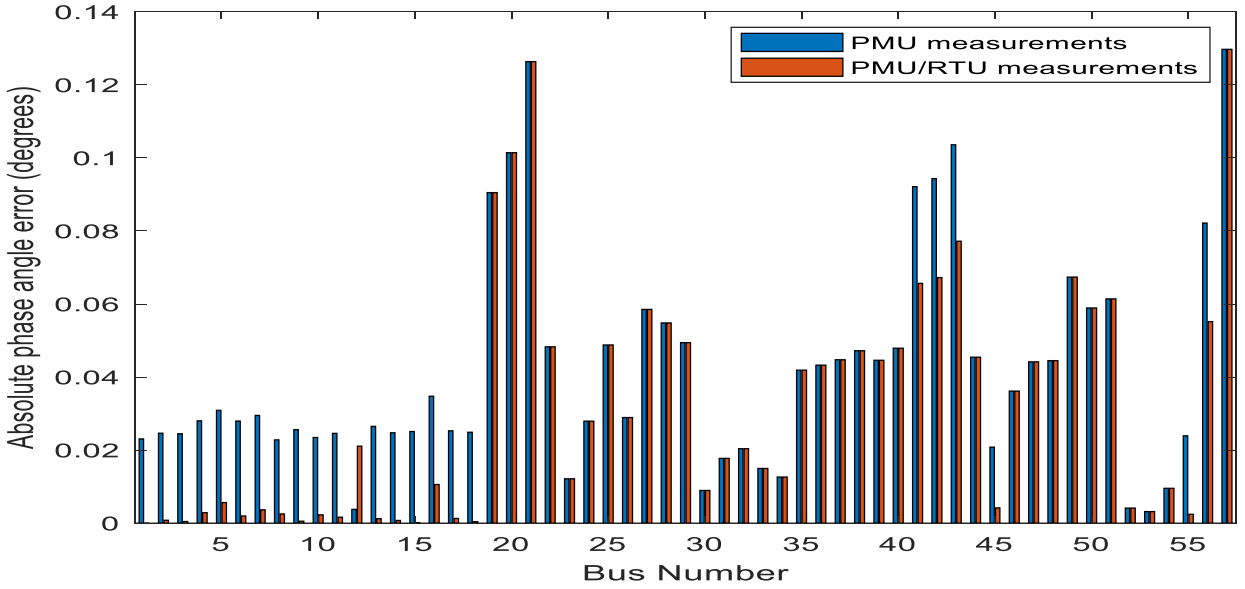

FIGURE 7. Absolute phase angle error for IEEE 57-bus.

TABLE 14. IEEE 14-bus reference and estimated values considering PMU loss at bus 6.

Bus number	Reference voltage magnitude	Estimated voltage magnitude using PMU measurements	Estimated voltage magnitude using PMU/RTU measurements	Reference phase angle	Estimated phase angle using PMU measurements	Estimated phase angle using PMU/RTU measurements
1	1.0600	1.0592	1.0592	0.0000	-0.0241	0.0001
2	1.0450	1.0443	1.0442	-4.9826	-5.0126	-4.9882
3	1.0100	1.0093	1.0092	-12.7251	-12.7668	-12.7422
4	1.0177	1.0170	1.0169	-10.3129	-10.3360	-10.3113
5	1.0195	1.0187	1.0187	-8.7739	-8.8052	-8.7804
6	1.0700	**0.0000**	1.0692	-14.2209	**0.0000**	-14.2121
7	1.0615	1.0606	1.0605	-13.3596	-13.3722	-13.3482
8	1.0900	1.0891	1.0890	-13.3596	-13.3776	-13.3542
9	1.0559	1.0551	1.0550	-14.9385	-14.9531	-14.9292
10	1.0510	1.0503	1.0501	-15.0973	-15.1119	-15.0879
11	1.0569	**0.0000**	1.0561	-14.7906	**0.0000**	-14.7818
12	1.0552	**0.0000**	1.0544	-15.0756	**0.0000**	-15.0671
13	1.0504	**0.0000**	1.0496	-15.1563	**0.0000**	-15.1481
14	1.0355	1.0348	1.0347	-16.0336	-16.0519	-16.0277

The PMU located at bus ten as per the topology given in figure 13, serves buses 6, 9, 10, 17, 20, 21, and 22. Buses 6, 9, 10, and 20 states are obtained since the buses are redundant, as shown in table 7. Using PMU/RTU measurements, all states are estimated due to redundancy provided by the RTU measurements in the event of a single PMU loss.

State estimation for IEEE 57-bus presents estimation results consistent with the other two test cases. A single PMU loss is initiated at bus 28 and the results presented in figures 16 and 17 indicate state estimation failure at buses 27, 28, and 29 when using PMU measurements only. PMU installed at bus 28 serves buses 27, 28, and 29, as shown in figure 18, and none of these buses is redundant, resulting in estimation failure. State estimation for this test case using PMU/RTU measurements gives estimation at all buses, further indicating the measurement

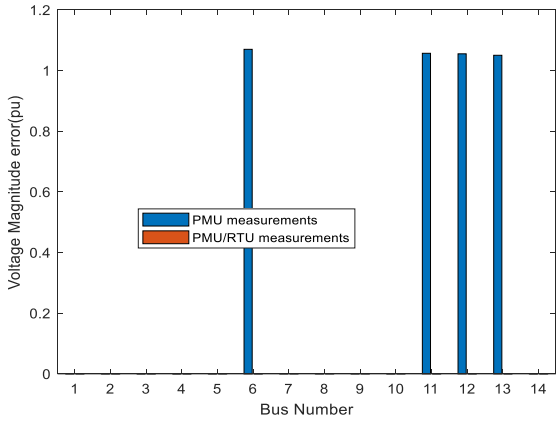

FIGURE 8. Voltage magnitude error for IEEE 14-bus considering single PMU loss at bus 6.

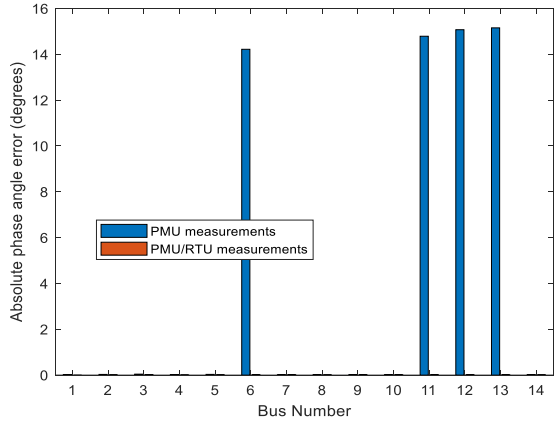

FIGURE 9. Absolute angle error for IEEE 14-bus considering single PMU loss at bus 6.

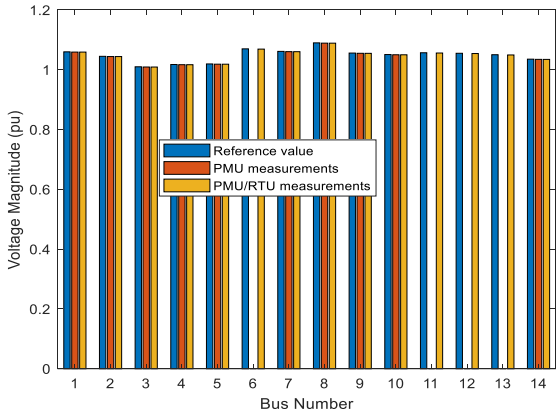

FIGURE 10. Comparison between reference values and estimated values for IEEE 14-bus voltage magnitude considering single PMU loss at bus 6.

redundancy provided by RTU measurements in state estimation.

For the overall evaluation of the estimator considering single PMU loss in each test case, the NCE value is determined. The results are shown in table 15, with an estimation based on

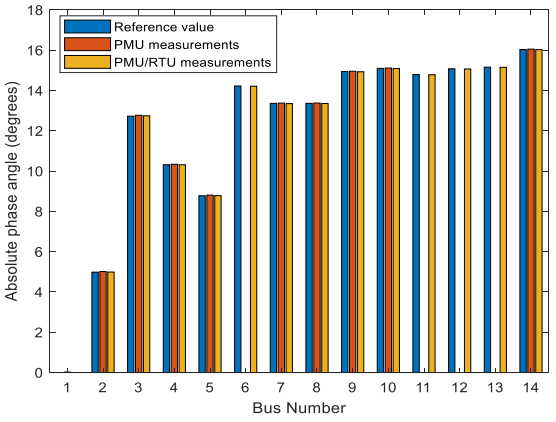

FIGURE 11. Comparison between reference values and estimated values for IEEE 14-bus absolute phase angle considering single PMU loss at bus 6.

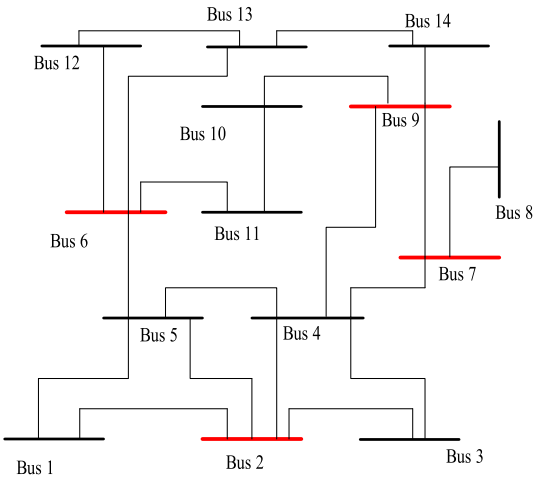

FIGURE 12. IEEE 14 -bus topology indicating buses installed with PMUs in red.

TABLE 15. NCE values considering single PMU loss.

System	PMU loss location	PMU/RTU measurements	PMU measurements
IEEE 14 BUS	Bus 6	0.42×10^{-2}	227.54×10^{-2}
IEEE 30 BUS	Bus 10	0.89×10^{-2}	22.96×10^{-2}
IEEE 57 BUS	Bus 28	1.35×10^{-2}	32.68×10^{-2}

PMU measurements only giving a high NCE value for all test cases. The high NCE value is attributed to estimation failure at the unobservable buses resulting in a high estimation error at such buses. Estimation based on hybrid PMU/ RTU measurements presents relatively low NCE values indicating high estimation accuracy resulting from measurement redundancy provided by RTU measurements. The computational time for state estimation considering single PMU loss is given in table 16.

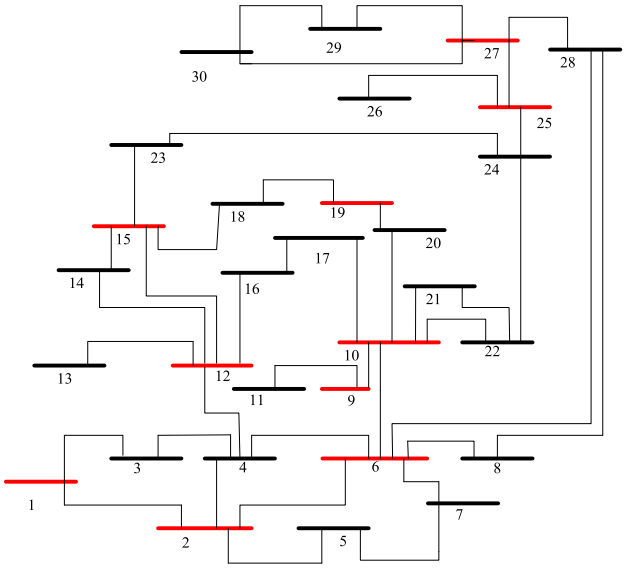

FIGURE 13. IEEE 30 -bus topology indicating buses installed with PMUs in red.

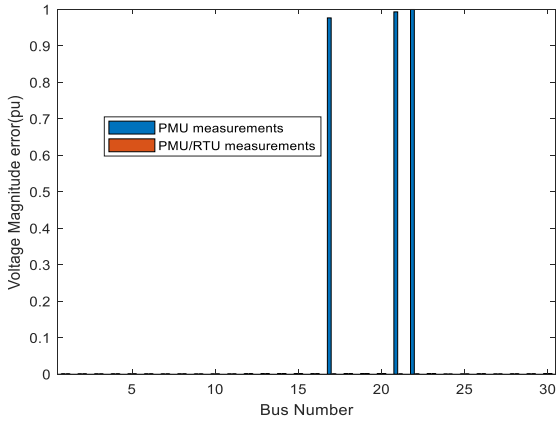

FIGURE 14. Voltage magnitude error for IEEE 30-bus considering single PMU loss at bus 10.

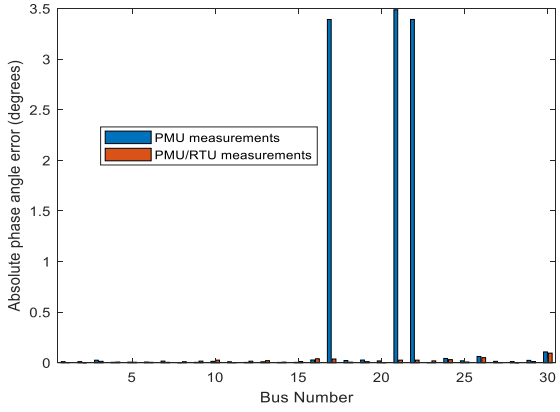

FIGURE 15. Absolute angle error for IEEE 30-bus considering single PMU loss at bus 10.

E. EVALUATION OF THE PROPOSED LHSE CONSIDERING BAD DATA EXISTENCE

The robustness of the proposed LHSE is tested by initiating bad data manually. In this paper, bad data is characterized

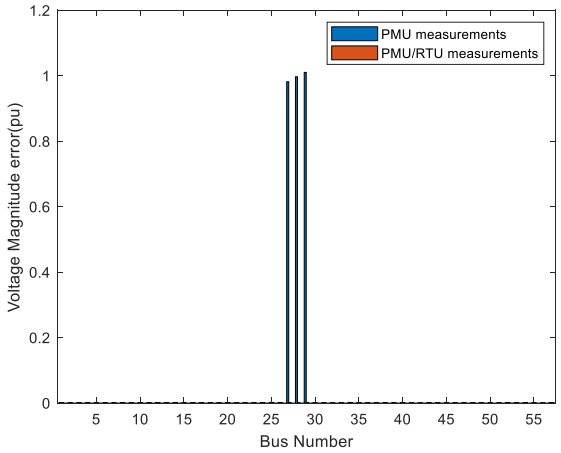

FIGURE 16. Voltage magnitude error for IEEE 57-bus considering single PMU loss at bus 28.

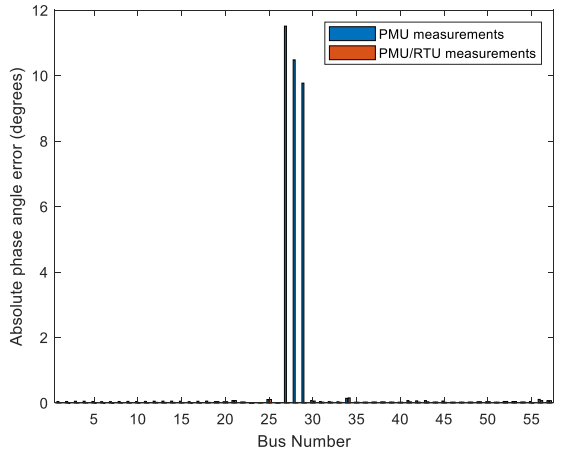

FIGURE 17. Absolute angle error for IEEE 57-bus considering single PMU loss at bus 28.

TABLE 16. State estimation computational time considering single PMU loss.

System	PMU/RTU measurements	PMU measurements
IEEE 14 BUS	0.002927 s	0.002154 s
IEEE 30 BUS	0.003130 s	0.003006 s
IEEE 57 BUS	0.004360 s	0.004099 s

by either measurement with a large standard deviation more than five times the normal deviation or negative values for the measurements [6]. A single bad data is introduced in both RTU and PMU measurement sets, as described in table 17 for the three test cases.

The performance of the proposed LHSE considering bad data is given in terms of NCE values in table 18. The NCE values obtained show a small or no deviation when the measurement sets contain bad data. Therefore, the robustness of the WLAV estimation criterion is depicted in the results obtained. The corresponding state estimation computation time considering bad data existence is given in table 19.

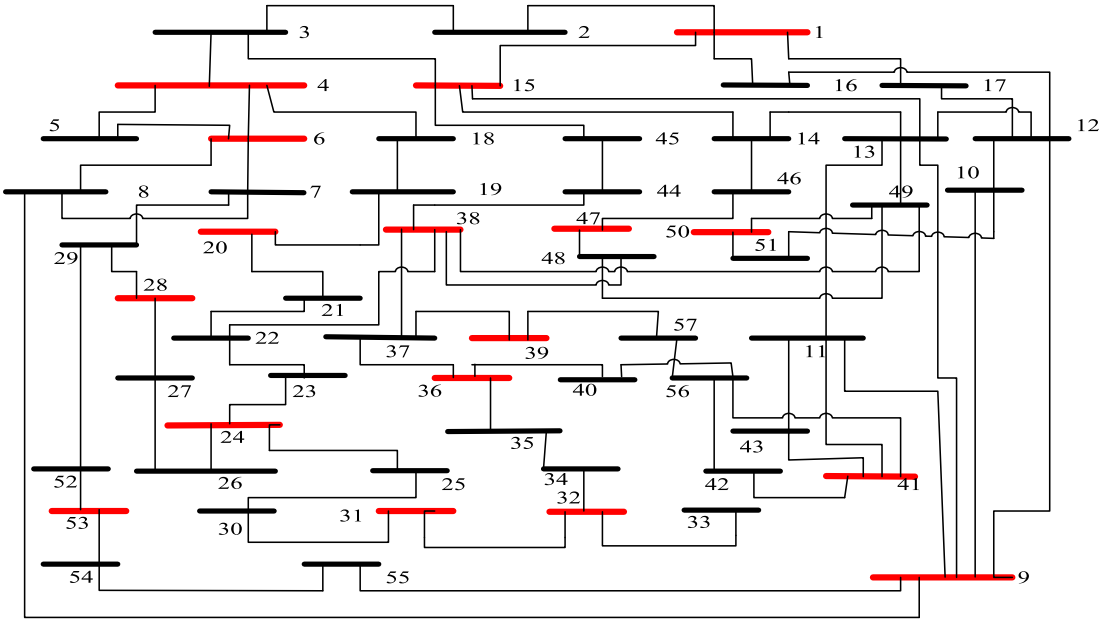

FIGURE 18. IEEE 57 -bus topology indicating buses installed with PMUs in red.

TABLE 17. Bad data integration into the measurement sets.

System	RTU measurement set	PMU measurement set
IEEE 14-BUS	A negative voltage magnitude value at bus 13	The real part of the current phasor value from bus 6 to bus 13 is integrated with a large standard deviation
IEEE 30-BUS	The voltage magnitude value at bus 1 is integrated with a large standard deviation	A negative voltage magnitude value at bus 6
IEEE 57-BUS	The voltage magnitude value at bus 1 is integrated with a large standard deviation	A negative voltage magnitude value at bus 6

TABLE 18. NCE values considering bad data existence.

System	Measurement set	PMU/RTU measurements	PMU measurements
IEEE 14 BUS	Without bad data	0.0051	0.0113
	With bad data	0.0204	0.0248
IEEE 30 BUS	Without bad data	0.0087	0.0144
	With bad data	0.0087	0.0140
IEEE 57 BUS	Without bad data	0.0164	0.0210
	With bad data	0.0166	0.0211

TABLE 19. State estimation computational time considering bad data existence.

System	PMU/RTU measurements	PMU measurements
IEEE 14 BUS	0.002269 s	0.002086 s
IEEE 30 BUS	0.003377 s	0.003135 s
IEEE 57 BUS	0.004610 s	0.004471 s

V. CONCLUSION

This research proposes a linear hybrid state estimator capable of simultaneously utilizing PMU and RTU measurements. A major advantage is that it is linear, resulting in a non-iterative state estimation process eliminating challenges associated with nonlinear algorithms. The study also focuses on evaluating the estimator's performance in the presence of either PMU measurements only or a combination of PMU and RTU measurements. The evaluation is performed on three standard test case systems assumed to have enough existing RTU meters for complete system observability. PMU inclusion in the system is based on optimal placement based on the ABC algorithm, a metaheuristic optimization algorithm with excellent exploration search techniques. The proposed LHSE model offers several advantages since the system observability, and linearity are guaranteed whether in the presence of measurements from RTU only, a combination of RTU and PMU, or PMU measurements only. As hybrid estimators leverage both measurement types to improve estimation performance, the proposed LHSE approach leverages RTU and PMU measurements to address PMU loss contingency. The proposed approach looks into system reliability against a single PMU loss contingency from a hybrid measurement perspective and not PMU measurements only. Based on the results obtained, the presence of RTU measurements mitigates single PMU loss effects. The estimator robustness against bad data is addressed by developing a WLAV estimation criterion.

The evaluation is inclined towards first establishing the effectiveness of the proposed LHSE and, secondly, the estimator's performance working with an optimal number of PMUs within the system and during a contingency such as PMU loss. The proposed estimator is also evaluated for robustness based on bad data existence. Simulation results indicate the effectiveness of hybrid measurements in state estimation, as shown by NCE values obtained for the different test cases. Measurement redundancy is key for state estimation. Therefore, system operators should consider integrating

existing RTU measurements with PMU measurements during the transition period and even in the future to address constraints such as cost and reliability. It is also prudent to install the relatively cheaper RTU meters for new power systems even if there are enough PMUs to make the system observable. Single PMU loss is a constraint widely explored in optimal PMU placement, which only increases the minimum number of PMUs required for observability. Based on simulation results obtained, PMU/RTU measurements address the single PMU loss, further minimizing the PMUs required in such contingency and reducing the infrastructural costs.

The future scope of this study will consider other constraints within the OPPP problem that always subject the problem to an increased number of PMUs for observability while working with the proposed LHSE.

REFERENCES

[1] A. Abur and A. G. Exposito, *Power System State Estimation: Theory and Implementation*. New York, NY, USA: Marcel Dekker, 2004.
[2] A. Monti, C. Muscas, and F. Ponci, *Phasor Measurement Units and Wide Area Monitoring Systems: From the Sensors to the System*, 1st ed. Amsterdam, The Netherlands: Elsevier, 2016.
[3] J. De La Ree, V. Centeno, J. S. Thorp, and A. G. Phadke, "Synchronized phasor measurement applications in power systems," *IEEE Trans. Smart Grid*, vol. 1, no. 1, pp. 20–27, Jun. 2010.
[4] S. Chakrabarti, E. Kyriakides, G. Ledwich, and A. Ghosh, "Inclusion of PMU current phasor measurements in a power system state estimator," *IET Gener., Transmiss. Distrib.*, vol. 4, no. 10, pp. 1104–1115, 2010.
[5] N. M. Manousakis, G. N. Korres, and P. S. Georgilakis, "Optimal placement of phasor measurement units: A literature review," in *Proc. 16th Int. Conf. Intell. Syst. Appl. Power Syst.*, Sep. 2011, pp. 1–6.
[6] A. Mukhtar, *Power System State Estimation*. Norwood, MA, USA: Artech House, 2013.
[7] M. Laouamer, R. D. Mohammedi, A. Kouzou, and A. Tlemcani, "Optimal placement of PMUs in Algerian network using genetic algorithm," in *Proc. 15th Int. Multi-Conf. Syst., Signals Devices (SSD)*, Mar. 2018, pp. 947–951.
[8] S. S. Noureen, V. Roy, and S. B. Bayne, "Phasor measurement unit integration: A review on optimal PMU placement methods in power system," in *Proc. IEEE Region 10 Hum. Technol. Conf. (R10-HTC)*, Dec. 2017, pp. 328–332.
[9] H. Daryabar, M. Moradi-Sepahvand, and T. Amraee, "Optimal placement of phasor measurement units for observability of Mazandaran transmission and sub-transmission networks," in *Proc. Smart Grid Conf. (SGC)*, Nov. 2018, pp. 1–6.
[10] E. O. Okendo, C. W. Wekesa, and M. J. Saulo, "Optimal placement of phasor measurement unit considering system observability redundancy index: Case study of the Kenya power transmission network," *Heliyon*, vol. 7, no. 7, Jul. 2021, Art. no. e07670.
[11] M. M. Ahmed and K. Imran, "An optimal PMU placement against N-1 contingency of PMU using integer linear programming approach," in *Proc. Int. Conf. Appl. Eng. Math. (ICAEM)*, Aug. 2019, pp. 127–132.
[12] K. B. Krishna, K. M. Rosalina, and N. Ramaraj, "Complete and incomplete observability analysis by optimal PMU placement techniques of a network," *J. Electr. Eng. Technol.*, vol. 13, no. 5, pp. 1814–1820, 2018.
[13] M. Zhou, V. Centeno, J. Thorp, and A. Phadke, "An alternative for including phasor measurements in state estimators," *IEEE Trans. Power Syst.*, vol. 21, no. 4, pp. 1930–1937, Nov. 2006.
[14] R. Baltensperger, A. Loosli, H. Sauvain, M. Zima, G. Andersson, and R. Nuqui, "An implementation of two-stage hybrid state estimation with limited number of PMU," in *Proc. IET Conf. Publications*, 2010, pp. 1–5.
[15] N. M. Manousakis, G. N. Korres, J. N. Aliprantis, G. P. Vavourakis, and G.-C.-J. Makrinas, "A two-stage state estimator for power systems with PMU and SCADA measurements," in *Proc. IEEE Grenoble Conf. PowerTech (POWERTECH)*, Jun. 2013, pp. 1–6.
[16] S. M. Khamis and N. H. Abbasy, "Enhanced performance of developed two-step (hybrid/PMU) linear state estimator model," *Int. J. Model. Optim.*, pp. 192–197, Aug. 2019.
[17] M. Göl and A. Abur, "A hybrid state estimator for systems with limited number of PMUs," *IEEE Trans. Power Syst.*, vol. 30, no. 3, pp. 1511–1517, May 2015.
[18] J. Hazra, K. Das, B. K. S. Roy, M. Padmanaban, and A. K. Sinha, "Multi-stage optimal PMU placement for hybrid state estimation," in *Proc. IEEE Power Energy Soc. Gen. Meeting*, Jul. 2017, pp. 1–5.
[19] G. A. Ortiz, D. G. Colome, and J. J. Q. Puma, "State estimation of power system based on SCADA and PMU measurements," in *Proc. IEEE ANDESCON*, Oct. 2016, pp. 1–4.
[20] N. M. Manousakis and G. N. Korres, "A hybrid power system state estimator using synchronized and unsynchronized sensors," *Int. Trans. Electr. Energy Syst.*, vol. 28, no. 8, pp. 1–19, 2018.
[21] M. Asprou, S. Chakrabarti, and E. Kyriakides, "A two-stage state estimator for dynamic monitoring of power systems," *IEEE Syst. J.*, vol. 11, no. 3, pp. 1767–1776, Sep. 2017.
[22] Y. Guo, B. Zhang, W. Wu, and H. Sun, "Multi-time interval power system state estimation incorporating phasor measurements," in *Proc. IEEE Power Energy Soc. Gen. Meeting*, Jul. 2015, pp. 1–5.
[23] M. Gol, A. Abur, and F. Galvan, "Rapid tracking of bus voltages using synchro-phasor assisted state estimator," in *Proc. 4th IEEE/PES Innov. Smart Grid Technol. Eur. (ISGT Europe)*, Oct. 2013, pp. 1–5.
[24] M. Asprou and E. Kyriakides, "Enhancement of hybrid state estimation using pseudo flow measurements," in *Proc. IEEE Power Energy Soc. Gen. Meeting*, Jul. 2011, pp. 1–7.
[25] J. Chen and A. Abur, "Placement of PMUs to enable bad data detection in state estimation," *IEEE Trans. Power Syst.*, vol. 21, no. 4, pp. 1608–1615, Nov. 2006.
[26] G. Valverde, S. Chakrabarti, E. Kyriakides, and V. Terzija, "A constrained formulation for hybrid state estimation," *IEEE Trans. Power Syst.*, vol. 26, no. 3, pp. 1102–1109, Aug. 2011.
[27] G. Korres and N. Manousakis, "State estimation and bad data processing for systems including PMU and SCADA measurements," *Electr. Power Syst. Res.*, vol. 81, no. 7, pp. 1514–1524, 2011.
[28] T. S. Bi, X. H. Qin, and Q. X. Yang, "A novel hybrid state estimator for including synchronized phasor measurements," *Electr. Power Syst. Res.*, vol. 78, no. 8, pp. 1343–1352, 2008.
[29] J. Zhao, G. Zhang, K. Das, G. N. Korres, N. M. Manousakis, A. K. Sinha, and Z. He, "Power system real-time monitoring by using PMU-based robust state estimation method," *IEEE Trans. Smart Grid*, vol. 7, no. 1, pp. 300–309, Jan. 2016.
[30] A. S. Dobakhshari, S. Azizi, M. Abdolmaleki, and V. Terzija, "Linear LAV-based state estimation integrating hybrid SCADA/PMU measurements," *IET Gener., Transmiss. Distrib.*, vol. 14, no. 8, pp. 1583–1590, Apr. 2020.
[31] A. S. Dobakhshari, M. Abdolmaleki, V. Terzija, and S. Azizi, "Robust hybrid linear state estimator utilizing SCADA and PMU measurements," *IEEE Trans. Power Syst.*, vol. 36, no. 2, pp. 1264–1273, Mar. 2021.
[32] A. Jovicic, M. Jereminov, L. Pileggi, and G. Hug, "A linear formulation for power system state estimation including RTU and PMU measurements," in *Proc. IEEE PES Innov. Smart Grid Technol. Eur. (ISGT-Europe)*, Sep. 2019, pp. 1–5.
[33] A. Jovicic and G. Hug, "Linear state estimation and bad data detection for power systems with RTU and PMU measurements," pp. 1–7, 2020, *arXiv:2001.10764*.
[34] S. P. Singh and S. P. Singh, "A novel multi-objective PMU placement method for power system state estimation," in *Proc. Int. Electr. Eng. Congr. (iEECON)*, Mar. 2018, pp. 1–4.
[35] B. Xu and A. Abur, "Observability analysis and measurement placement for systems with PMUs," in *Proc. IEEE PES Power Syst. Conf. Expo.*, Oct. 2004, vol. 2, no. 1, pp. 943–946.
[36] A. Almunif and L. Fan, "Mixed integer linear programming and nonlinear programming for optimal PMU placement," in *Proc. North Amer. Power Symp. (NAPS)*, Sep. 2017, p. 5.
[37] G. C. Patil and A. G. Thosar, "Optimal placement of PMU for power system observability using integer programming," in *Proc. Int. Conf. Innov. Res. Electr. Sci. (IICIRES)*, Jun. 2017, pp. 1–6.
[38] A. Aziz G. Mabaning and J. Rel C. Orillaza, "Complete solution of optimal PMU placement using reduced exhaustive search," in *Proc. IEEE Region 10 Conf. (TENCON)*, Nov. 2016, pp. 823–826.
[39] F. Zeng, H. Xu, D. Zhang, X. Zhang, and Y. Yuan, "A new strategy for optimal PMU placement based on limited exhaustive approach," in *Proc. Int. Conf. Power Syst. Technol. (POWERCON)*, Oct. 2014, pp. 67–74.
[40] M. U. Usman and M. O. Faruque, "Applications of synchrophasor technologies in power systems," *J. Mod. Power Syst. Clean Energy*, vol. 7, no. 2, pp. 211–226, Mar. 2019.

[41] M. Shahriar, I. Habiballah, and H. Hussein, "Optimization of phasor measurement unit (PMU) placement in supervisory control and data acquisition (SCADA)-based power system for better state-estimation performance," *Energies*, vol. 11, no. 3, p. 570, Mar. 2018.
[42] R. D. Zimmerman, C. E. Murillo-Sánchez, and R. J. Thomas, "MATPOWER: Steady-state operations, planning and analysis tools for power systems research and education," *IEEE Trans. Power Syst.*, vol. 26, no. 1, pp. 12–19, 2011, doi: 10.1109/TPWRS.2010.2051168.
[43] V. Murugesan, Y. Chakhchoukh, V. Vittal, G. T. Heydt, N. Logic, and S. Sturgill, "PMU data buffering for power system state estimators," *IEEE Power Energy Technol. Syst. J.*, vol. 2, no. 3, pp. 94–102, Sep. 2015.
[44] R. F. Nuqui and A. G. Phadke, "Phasor measurement unit placement techniques for complete and incomplete observability," *IEEE Trans. Power Del.*, vol. 20, no. 4, pp. 2381–2388, Oct. 2005.
[45] X. Chen, F. Wei, S. Cao, C. B. Soh, and K. J. Tseng, "PMU placement for measurement redundancy distribution considering zero injection bus and contingencies," *IEEE Syst. J.*, vol. 14, no. 4, pp. 5396–5406, Dec. 2020.
[46] A. Kulanthaisamy, R. Vairamani, N. K. Karunamurthi, and C. Koodalsamy, "A multi-objective PMU placement method considering observability and measurement redundancy using ABC algorithm," *Adv. Electr. Comput. Eng.*, vol. 14, no. 2, pp. 117–128, 2014.
[47] M. Mernik, S.-H. Liu, D. Karaboga, and M. Črepinšek, "On clarifying misconceptions when comparing variants of the artificial bee colony algorithm by offering a new implementation," *Inf. Sci.*, vol. 291, pp. 115–127, Jan. 2015.
[48] S. Aslan, "A transition control mechanism for artificial bee colony (ABC) algorithm," *Comput. Intell. Neurosci.*, vol. 2019, pp. 1–24, Apr. 2019.
[49] D. Karaboga and B. Akay, "A comparative study of artificial bee colony algorithm," *Appl. Math. Comput.*, vol. 214, no. 1, pp. 108–132, 2009.
[50] M. S. Shahriar and I. O. Habiballah, "Least measurement rejected algorithm for robust power system state estimation," in *Proc. IEEE Innov. Smart Grid Technol. Asia (ISGT-Asia)*, Dec. 2017, pp. 1–6.
[51] L. A. Azzeddine, M. R. Djamel, K. Abdellah, and R. M. Mounir, "Optimal PMU placement in power system based on multi-objective particle swarm optimization," in *Proc. 15th Int. Multi-Conf. Syst., Signals Devices (SSD)*, Mar. 2018, pp. 941–946.
[52] I. Abdulrahman and G. Radman, "ILP-based optimal PMU placement with the inclusion of the effect of a group of zero-injection buses," *J. Control, Autom. Electr. Syst.*, vol. 29, no. 4, pp. 512–524, Aug. 2018.
[53] A. Raj and C. Venkaiah, "Optimal PMU placement by teaching-learning based optimization algorithm," in *Proc. 39th Nat. Syst. Conf. (NSC)*, Dec. 2015, pp. 1–6.
[54] K. A. Jeyaraj, V. Rajasekaran, S. K. N. Kumar, and K. Chandrasekaran, "A multi-objective placement of phasor measurement units considering observability and measurement redundancy using firefly algorithm," *J. Electr. Eng. Technol.*, vol. 10, no. 2, pp. 474–486, Mar. 2015.
[55] Y. Azzougui, A. Recioui, and A. Mansouri, "PMU optimal placement in wide area monitoring systems using grey wolf optimization technique," *Algerian J. Signals Syst.*, vol. 4, no. 1, pp. 1–7, Jun. 2019.

MERCY NDINDA KIIO (Student Member, IEEE) received the Bachelor of Science degree in electrical and electronic engineering and the Master of Science degree in electrical engineering from the Jomo Kenyatta University of Agriculture and Technology, Kenya, in 2010 and 2017, respectively. She is currently pursuing the Ph.D. degree in electrical engineering with the Pan African University Institute for Basic Sciences, Technology, and Innovation, Kenya. Her research interests include power system state estimation, power system control, and renewable energy development.

CYRUS WABUGE WEKESA received the B.Sc. and M.Sc. degrees from the University of Nairobi, Nairobi, Kenya, and the Ph.D. degree from Tokushima University, Tokushima, Japan, all in electrical engineering. Currently, he is an Associate Professor with the School of Engineering, University of Eldoret. Previously, he has taught at the Jomo Kenya University of Agriculture and Technology and the University of Nairobi. He is a pioneer Researcher in renewable energy sources for electrification in Kenya and has published papers. He has successfully supervised more than 20 M.Sc./Ph.D. students. His research interests include electrical power systems, distributed energy resources, demand side management, demand response, and energy management.

STANLEY IRUNGU KAMAU (Member, IEEE) received the bachelor's degree in electrical engineering from Moi University, Kenya, in 1990, the M.Eng.Sc. degree in electrical engineering from the University of New South Wales, Australia, in 1993, and the Dr.Ing. degree in electrical engineering from Ruhr-Universität Bochum, Germany, in 2004. He is currently an Associate Professor with the Department of Electrical and Electronic Engineering, Jomo Kenyatta University of Agriculture and Technology, Kenya. His research interests include hybrid control systems, real-time control, power system state estimation and control, and renewable energy development.